Radiative states in type-II GaSb/GaAs quantum wells

N. N. Ledentsov,* J. Böhrer, M. Beer, F. Heinrichsdorff, M. Grundmann, and D. Bimberg
Institut für Festkörperphysik, Technische Universität Berlin, Hardenbergstrasse 36, D-10623 Berlin, Germany

S. V. Ivanov, B. Ya. Meltser, S. V. Shaposhnikov, I. N. Yassievich, N. N. Faleev, P. S. Kop'ev, and Zh. I. Alferov
A. F. Ioffe Physical Technical Institute, 194021, Politekhnicheskaya 26, St. Petersburg, Russia
(Received 24 February 1995; revised manuscript received 5 July 1995)

We have studied optical properties of staggered band line-up (type-II) heterostructures based on strained GaSb sheets in a GaAs matrix. The giant valence-band offset characteristic to this heterojunction leads to an effective localization of holes in ultrathin GaSb layers. An intense photoluminescence (PL) line caused by radiative recombination of localized holes with electrons located in the nearby GaAs regions is observed. The separation of nonequilibrium electrons and holes in real space results in a dipole layer and, thus, in the formation of quantum wells for electrons in the vicinity of the GaSb layer. The luminescence maximum shifts towards higher photon energies with rising excitation density reflecting the increase in the electron quantization energy. A bimolecular recombination mechanism is revealed in PL and in time-resolved PL studies. In the case of pseudomorphic monolayer-thick GaSb layers, the radiative exciton ground state does not exist. Accordingly, small absorption coefficients and a featureless behavior of the band-to-band calorimetric absoprtion spectrum are found in the vicinity of $k_{x,y}=0$. Remarkable enhancement of the absorption coefficient with a characteristic onset is observed for heavy holes with $k_{x,y}>0$. Radiative states in the continuum of heavy-hole subbands are revealed also in temperature-dependent PL studies. The experimentally measured onset energies point out the importance of GaSb heavy- and light-hole mixing effects. We demonstrate intense luminescence from staggered band line-up GaSb-GaAs heterostructures up to room temperature.

I. INTRODUCTION

Recent interest in staggered line-up heterostructures composed of direct-band-gap materials originates from the unique properties characteristic to these systems.[1–3] Spatial separation of two-dimensional electrons and holes at the interface results in a tunability of their optical properties,[4,5] while quantum-mechanical tunneling at abrupt interfaces allows for effective overlapping of their wave functions, resulting in exciton oscillator strengths and optical transition matrix elements comparable in optimized structure geometry to those of type-I quantum wells.[6] Staggered band alignment thus gives a possibility to realize optical emission with a photon energy much smaller than the band-gap energy of each of the semiconductors forming a heterojunction. In the case of heterojunctions with a broken line-up (e.g., InAs/GaSb), the radiative recombination energy may be chosen within the whole far-infrared optical range.[2,7–10] Type-II structures thus offer possibilities both in fundamental physics[11,12] and for device applications which cannot be realized with type-I quantum wells in the III-V material system. However, despite the demonstration of an injection laser based on a type-II heterojunction,[4] practical applications of these structures are still hampered by a poor understanding of their fundamental properties and the few actual systems which were experimentally explored up to now.

In this work we have studied the electronic spectrum and optical properties of type-II heterostructures based on GaSb sheets in a GaAs matrix grown by molecular-beam epitaxy. This heterojunction can be considered a model system for studying the optical properties of a particular class of type-II structures. Large hole localization energies due to the giant valence-band offset in this system may result in practical applications for light-emitting devices grown on GaAs substrates in the spectral range of 1–1.5 μm. We demonstrate the tunability of the optical properties of this system due to nonequilibrium carrier-induced dipole-layer formation. In contrast to type-I quantum wells, optical absorption and luminescence efficiency are found to be strongly influenced by heavy- and light-hole mixing effects. At several points in the paper we will compare the results for GaSb/GaAs with those for ultrathin InAs/GaAs layers in order to point out the specific differences to a type-I system.

II. GROWTH AND CHARACTERIZATION

Samples were grown by elemental source molecular-beam epitaxy (MBE) on GaAs(100) substrates using a RIBER-32 MBE machine. Growth rates were 0.8 μm/h for GaAs and GaSb. Arsenic and antimony vapor pressures were $2-3\times10^{-4}$ Pa. After oxide desorption, a 0.5-μm-thick GaAs buffer was grown at 600 °C. Then growth was interrupted until the substrate had cooled down to 470 °C. Subsequently, the surface was exposed to Sb flux, and the desired amount of GaSb was deposited. The GaSb layer was regrown with a GaAs cap. In this work we have studied single ultrathin GaSb layers in the GaAs matrix, as well as multilayer GaSb-GaAs structures. Reflection high-energy electron-diffraction (RHEED) patterns were monitored during the growth process.

Photoluminescence (PL) was excited using the 632.8- and 514.5-nm lines of He-Ne and Ar^+-ion lasers, respec-

tively, and detected using a cooled germanium *p-i-n* photodetector. PL measurements were performed in the temperature range of 2–300 K, and the intensity range of 0.01–500 W cm^{-2}, respectively.

Calorimetric absorption (CAS) spectroscopy was used to characterize the electronic spectrum of the structures grown. The CAS signal is caused by the part of the photoexcited electron-hole pairs recombining nonradiatively and emitting phonons. The CAS experiments were carried out at $T=500$ mK, where particularly high sensitivity is realized. Minimal detectable αd products were as low as 10^{-5} for excitation by a broad-spectrum lamp light dispersed through a 1-m monochromator. Second derivative CAS spectra were used used for measuring optical transition energies with large precision. Details of the experimental setup are published elsewhere.[13,14]

The structural properties were investigated using a double-crystal x-ray diffractometer. Differential x-ray-diffraction studies[15] revealed the good structural quality of GaSb/GaAs structures. Rocking curves were measured for (004) reflection using Cu $K_{\alpha 1}$ radiation.

Two model GaSb/GaAs superlattice systems were studied: with intentionally deposited GaSb layers (*A*) and with GaSb layers formed due to As to Sb exchange reactions during the growth interruption under Sb flux (*B*). A rocking curve of sample *A* is shown in Fig. 1. The period of superlattice *A* was derived from the well-resolved satellite peaks to be equal to 440±10 Å, in agreement with the calibrated GaAs growth rate. The average relative lattice parameter change in growth direction caused by the GaSb/GaAs superlattice was equal to 0.0214±0.0019. This corresponds to a GaSb concentrtion averaged within one period of 2.54% and, thus, the effective width of each GaSb layer equals 11.2±0.05 Å assuming a pseudomorphic GaSb layer. From this amount only 4.7 Å of GaSb were deposited intentionally, according to the calibrated GaAs growth rate. Thus the remaining 6.5 Å of GaSb were formed during the 30-s growth interruption under Sb_4 flux prior to each intentional GaSb deposition cycle. A similar analysis of the data for the GaSb/GaAs superlattice *B* with a period of 85 Å grown without any intentional GaSb deposition but the 10-s growth interruption under Sb_4 flux performed after each GaAs deposition cycle have shown that the effective width of the GaSb layers formed under these conditions equals 3.17 Å. Thus we conclude that *a complete* GaSb *monolayer* forms at 470 °C within 10 s under Sb flux. Formation of a *second* GaSb monolayer occurs within an additional 15–20 s. Further increase of growth interruption time does not result in a significant increase of GaSb layer thickness. We also found no evidence of unintentional GaSb layer formation with growth interruptions under Sb flux at 550 °C. The latter may probably be attributed to effective GaSb evaporation at high temperatures stimulated by strain in the GaSb pseudomorphic layer.

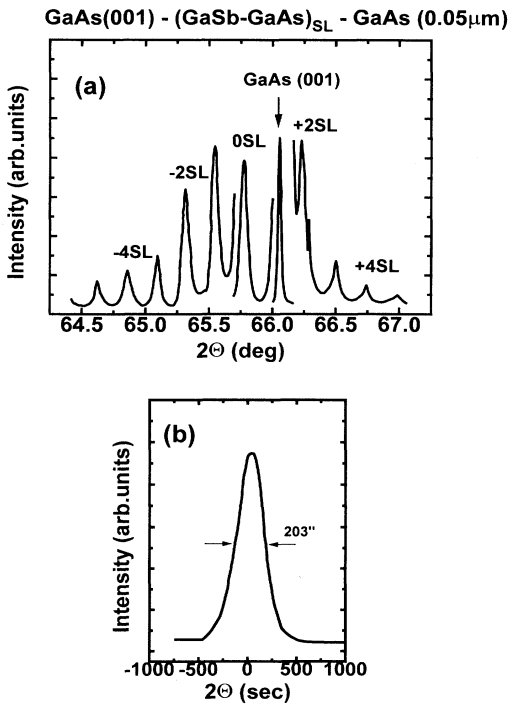

FIG. 1. Double-crystal x-ray-diffraction curves of the GaSb-GaAs superlattice (superlattice *A*): (a) coherent rocking curve, (b) Θ curve.

III. THEORETICAL CONSIDERATIONS

A. Band lineup

In order to obtain a realistic approximation of the band line-up at our GaSb/GaAs heterojunction, we follow the procedure given in Ref. 16. There, self-consistent *ab initio* band-structure calculations were performed, and a common reference level for the constituents involved in heterojunctions was introduced, thus enabling the calculation of band offsets including strain effects. Parameters used for the calculation were chosen according to Ref. 17 except for temperature-dependent energy-band parameters which were taken near 4 K ($E_g^{GaAs}=1.519$ eV, $E_g^{GaSb}=0.81$ eV, and $\Delta_0^{GaSb}=0.75$ eV).[18] Strain in GaSb layers due to their ~7% lattice mismatch with the GaAs

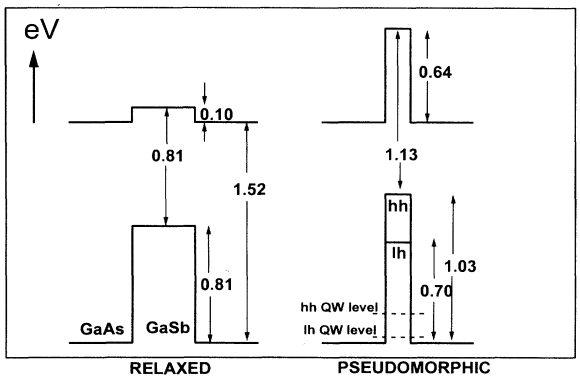

FIG. 2. Band alignment scheme for a GaSb/GaAs heterostructure of a completely relaxed (a) and a pseudomorphic GaSb layer (b) calculated from Ref. 16.

substrate has a dramatic effect on the energies of the top of the GaSb heavy- and light-hole subbands and on the energy of the bottom of the GaSb conduction band. The alignment of the conduction and valence bands of the pseudomorphic and fully relaxed cases are shown in Fig. 2. The unintentional doping level of the GaAs layers was as low as 10^{14}–10^{15} cm^{-3}; thus the band-bending effects are insignificant in our case. The relatively small spike in the conduction band resulting from the fully relaxed type-II GaSb/GaAs heterojunction (0.10 eV) is dramatically enhanced to 0.64 eV for compressive strain in GaSb pseudomorphic layers. The originally large valence-band offset (0.81 eV) is further enhanced to 1.03 eV. From these parameters, the localization energies calculated for heavy and light holes in a 3-Å pseudomorphic layer in the envelope-function approximation are 180 and 25 meV, respectively.

B. Excitons

One of the most important parameters which determine the optical properties of quantum-size heterostructures is the exciton binding energy. If the potential spike in the conduction band does not appreciably influence the electron and hole wave-function overlap (partial transparency of the conduction-band barrier due to its small thickness and the small electron effective mass), the exciton binding energy is expected to be comparable to its GaAs bulk value, i.e., 4.2 meV.[18] In the case of a remarkably low transparency of the barrier (large barrier height), on the other hand, the *s*-type exciton is not stable. In Fig. 3 we show the dependence of the exciton binding energies (*s*- and *p*-exciton states) on the dimensionless parameter κa_B which characterizes the transparency of the potential spike in this case. The parameters are defined below. Calculations were performed by the approach proposed in Ref. 19. This variational approach uses the zero radius potential method to describe exciton states in systems with very thin potential wells. According to this model, the exciton Schrödinger equation for a system with a thin potential spike reads

$$\left[-\frac{\hbar^2}{2m_e}\Delta-\frac{e^2}{\varepsilon_0 r}+\frac{\hbar^2}{m_e}\kappa\delta(z)\right]\Psi=E\Psi \tag{1a}$$

(the hole effective mass is assumed to be large compared to the electron effective mass). Here κ^{-1} is a localization length introduced in accordance with the interface boundary condition

$$\kappa=m_e V_0 L/\hbar^2 , \tag{1b}$$

V_0 is the conduction band barrier height; L the barrier width; m_e and ε_0 are the cladding material (GaAs) effective electron mass and dielectric constant, respectively, a_B is the three-dimensional Bohr exciton radius in GaAs; and $r=\sqrt{x^2+y^2+z^2}$. The Schrödinger equation is solved with a variational trial function of the form

$$\Psi=A\exp\left\{-\frac{\lambda r}{a_B}+\kappa|z|\right\} , \tag{2}$$

which results in the following equation for the variational parameter λ:

$$\lambda=1+\left[\frac{\kappa a_B}{2\lambda-\kappa a_B}\right]^2 . \tag{3}$$

The solutions of this equation are used to calculate the dependence of the binding energy on the parameter κa_B shown in Fig. 3 from

$$E_{\text{exc}}=2E_B\left[\lambda_0(1-\sqrt{\lambda_0-1})-\frac{\lambda_0^2}{2}\right] . \tag{4}$$

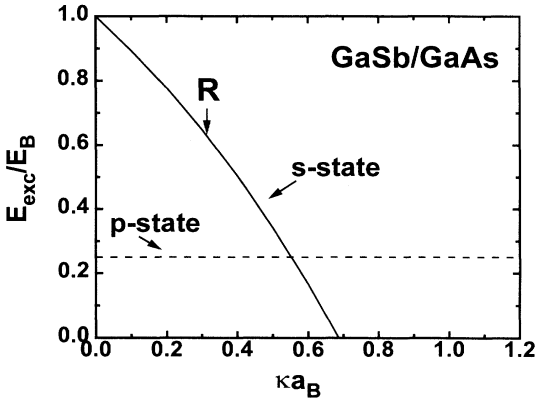

FIG. 3. GaSb exciton binding-energy dependence on the effective transparency κa_B of a GaSb-related potential spike in the conduction band (solid line). The dashed line indicates the *p* state. The arrow marks the calculated κa_B value for a completely relaxed (*R*) GaSb 1-ML-thick insertion.

The exciton binding energy turns out to be a very strong function of κa_B. This result is opposite to the results derived for the exciton binding energy in InAs monolayers in a GaAs matrix, where the potential spike in the conduction band attracts the electron[19] and the exciton binding energy significantly *increases* as compared to its bulk value. In type-II structures the exciton binding energy is found to *decrease* with increasing barrier height and width. In the theoretical case of a fully relaxed, 1-ML-thick GaSb layer, κa_B equals ~ 0.3 and the exciton binding energy is only slightly smaller as compared to the three-dimensional case. For the realistic situation of a pseudomorphic layer, κa_B is close to unity and *no* stable *s*-exciton ground state exists. The lowest exciton state becomes *p* type, having a fairly small binding energ (~ 1 meV), which is not affected by the occurrence of the potential spike in the conduction band. We emphasize that this behavior is expected for excitons involving both heavy and light holes.

Thus we conclude that for GaSb monolayers in a GaAs matrix the exciton binding energy, as well as electron and hole ($k=0$) wave-function overlap in real space, are negligibly small—the hole is strongly localized in the GaSb whereas the electron is spatially separated from the hole. In the case of finite k_z values the wave-function overlap gradually increases with $1/k_Z$, because electrons with larger k_Z values some closer to the localized holes.

C. Luminescence of nonequilibrium carriers

A nonexcitonic mechanism of a nonequilibrium carrier recombination being indirect in real space has to be considered in view of the observed high luminescence efficiency. The formation of a dipole layer populated with quantized nonequilibrium carriers close to the GaSb/GaAs interface at even moderate excitation intensities is responsible for this effect. The attractive potential of this layer forms a quantum well for nonequilibrium electrons, the quantization energy of which depends on the excitation intensity. An increase in the excitation density raises the steepness of the confining potential and, consequently, the electron quantization energy.[20]

The steady-state sheet concentrations of electrons n_W and holes p_W generated in the thin layer region by a photon flux I are characterized by the relation

$$n_W p_W = n_W^2 = \frac{\alpha I (L+l)^2}{\gamma} . \tag{5}$$

Here a denotes the absorption coefficient, L the width of the GaSb layer, l the multiple-quantum-well cladding layer thickness, and γ the radiative recombination coefficient. The strongly localized holes form a charged plane and, correspondingly, produce an approximately triangular well with an electric-field strength of

$$\varepsilon = \frac{2\pi e n_W}{\varepsilon_0} \propto \sqrt{I} . \tag{6}$$

The ground electron state in such a well is given by[21]

$$E_e = \text{const}\varepsilon^{2/3} \equiv bI^{1/3} , \tag{7}$$

with

$$b = \left[\frac{9\pi}{8}\right]^{2/3} \left[\frac{\hbar^2}{2m_e}\right]^{1/3} \left[\frac{2\pi e^2}{\varepsilon_0}\right]^{2/3} \left[\frac{\alpha(L+l)^2}{\gamma}\right]^{1/3} . \tag{8}$$

The electron quantization energy is thus expected to increase proportionally with the third root of the excitation density.

IV. OPTICAL CHARACTERIZATION

In Fig. 4 we show the photoluminescence (PL) spectra ($\lambda_{exc}=632.8$ nm) of several GaSb layers inserted into a GaAs matrix. The GaSb layer thicknesses are equal to 3, 8.5, and 11 Å. The incorporation of a GaSb monolayer results in the appearance of an intense line in the PL spectrum strongly shifted to lower energy with respect to the GaSb band gap. This line dominates the luminescence spectrum in the whole range of observation temperatures and excitation densities used in this work.

The dependence of the peak energy of the GaSb-related luminescence on the average thickness of the GaSb layer recorded at low excitation densities is shown in Fig. 5 with filled squares. PL peak energies of InAs layers of similar layer thicknesses are also shown in the same figure for comparison (filled circles). The localization energies calculated for heavy and light holes in the pseudomorphic 1-ML thick GaSb/GaAs quantum well are 180 and 25 meV, respectively. It can be seen that for structures with larger average GaSb layer thicknesses ($L>1$ ML) the calculated energies for the GaAs electron—GaSb heavy-hole transition are systematically below the experimentally observed ones. This indicates that the real heavy-hole localization energies are smaller than the theoretically predicted ones. The origin of this discrepancy observed for thicker GaSb layers is not clear; however, we note that for those samples both RHEED data and plan-view transmission electron microscopy images indicate that the GaSb layer becomes corrugated.

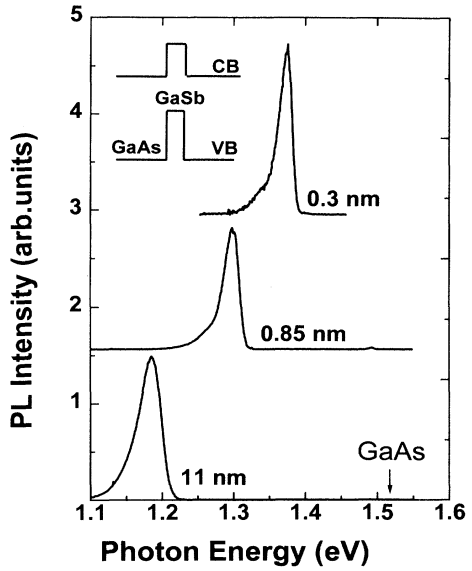

FIG. 4. Photoluminescence (PL) spectra (0.1 W/cm^{-2}, 8 K) of samples with different GaSb layer thicknesses. The GaSb band-gap energy is indicated by the arrow. The band alignment scheme of the structures studied is shown in the inset.

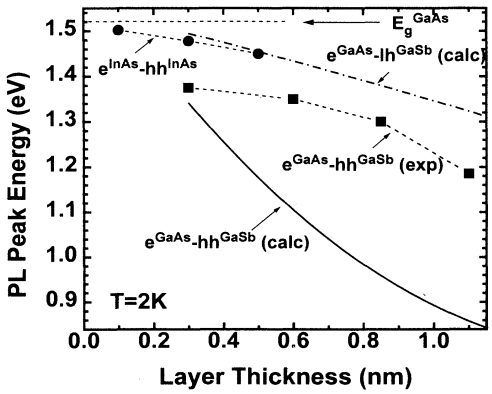

FIG. 5. PL peak energy dependence on the average thickness of the GaSb layer (squares). Luminescence peak energy for InAs insertions of the same thickness is shown for comparison (circles). Calculated positions for heavy- and light-hole exciton peaks are shown by solid and dashed-dotted lines, respectively. Excitation photon energy 1.959 eV, excitation density 1 W cm^{-2}.

This morphological instability finally results in the case of even thicker (> 12 Å) layers in the formation of GaSb three-dimensional (3D) islands (quantum dots) having a size of ~200 Å and a rectangular base.[22] Formation of the dots leads to an appearance of a second luminescence line, shifted to lower energy with respect to the residual two-dimensional wetting layer PL line.[22] This quantum dot PL line is not shown in Figs. 4 and 5. The complexity of the realistic GaSb/GaAs interface for average thicknesses of GaSb deposited exceeding 1 ML explain why the calculations based on a simple layer model are not valid. Interface corrugation-induced relaxation of the uniaxial strain (z) component reduces the potential well for heavy holes and increases the one for light holes.

Disagreement between experimentally observed and theoretically calculated PL energies for GaSb average layer thicknesses above 1 ML can be also explained by other effects, e.g., by segregation of Sb atoms. However, in this scenario the disagreement with theory should be more pronounced exactly for layers with *smaller* average thicknesses, as opposite to the experimental observations. In any case, possible formation of a *thin* intermixing-induced $GaAs_XSb_{1-X}$ layer does not *qualitatively* change the physical picture discussed, as the staggered band line-up alignment is also maintained for the $GaAs/GaAs_XSb_{1-X}$ heterojunction. The electron remains localized in the GaAs regions and the hole in the GaSb-rich regions in both models. Long-range Sb segregation resulting in full intermixing of the GaSb layers can be *excluded* in view of our x-ray and TEM data. More information on the dimensionality (quasi-2D or quasi-3D) of the electron at different excitation densities and on the origin of the transitions involved can be extracted from PL studies in a magnetic field directed parallel or perpendicular to the GaSb quantum-well plane.

In the small GaSb average thickness regime (~1 ML), where quantum-well model still works, GaSb insertions in a GaAs matrix result in a much stronger spectral shift of the luminescence line toward lower photon energies than InAs ones (see Fig. 5). Contrary to the InAs/GaAs case, only holes are localized in the GaSb layers, and the observed shift reflects the *hole localization energy* and its variation with thickness. Thus, the *hole localization energy* in the case of ultrathin (~1 ML) GaSb layers exceeds that of InAs layers of the same thickness by approximately one order of magnitude. This gives a possibility to reach the practically important 1.3–1.5-μm range, e.g., by stacking 1-ML-thick GaSb layers separating them by 1–2-ML-thick GaAs layers.

In Fig. 6(b) we show the PL spectra of 1-ML GaSb inserted into a GaAs matrix recorded at different excitation densities [the sketch of the structure is given in Fig. 6(a)]. With rising excitation density, the PL peak shifts toward higher energies. The shift of the PL maximum [see Fig. 6(c)] follows the expected behavior for the electron quantization energy, as is illustrated in Fig. 6(a). At the same time, the shape of the PL line does not change significantly with the excitation density. The total lifetime $[\tau_{tot}=(L+l)/n_W\gamma]$ of the nonequilibrium carriers may be derived by fitting the slope of the dependence shown in Fig. 7(c) which yields γ. The value of τ_{tot} obtained in such a manner equals 300–10 ns in the excitation density range 0.5–500 W cm^{-2}, respectively. These values are in reasonable agreement with typical initial decay constants of 100–2 ns observed in *time-resolved cathodoluminescence* studies at low and high excitation densities, respectively, which also reveal strongly nonexponential transients.

In Figs. 7(a) and 7(b) (note the logarithmic scale for PL and CAS spectra) we show the calorimetric absorption spectra measured at $T=500$ mK of the superlattice com-

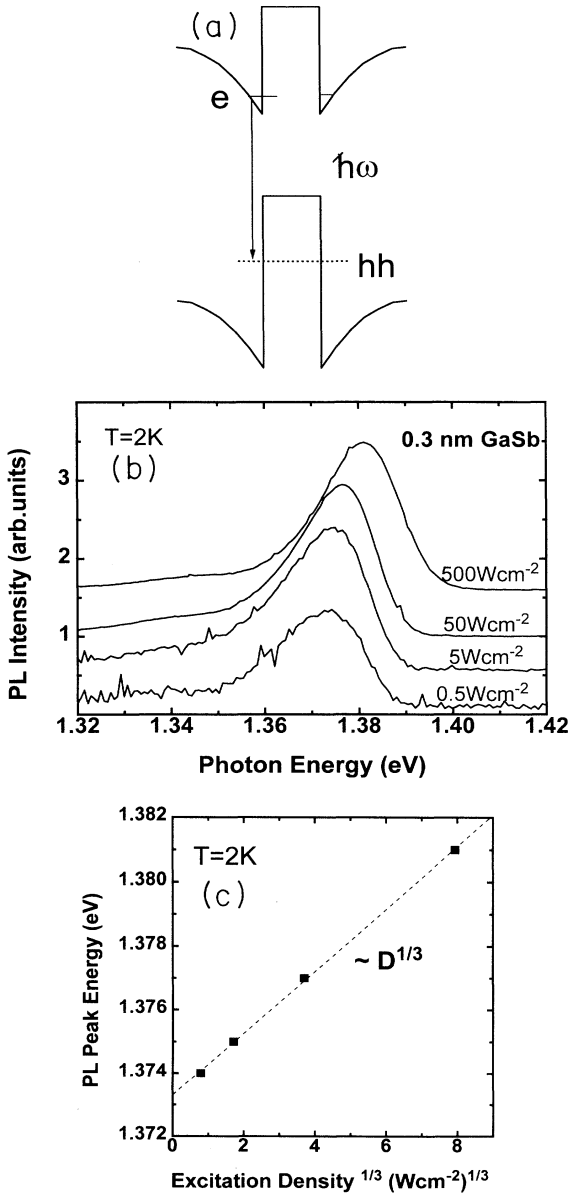

FIG. 6. (a) Sketch illustrating the modification of band alignment caused by nonequilibrium carriers. (b) PL spectra of a GaSb/GaAs superlattice B composed of 1-ML-thick GaSb layers recorded at 1.6 K at different excitation densities. (c) PL peak energy dependence on the cubic root of the excitation density.

posed of GaSb layers with average layer thicknesses of 3 Å [Fig. 7(a)], and of the superlattice composed of 11-Å-thick GaSb layers [Fig. 7(b)]. Second derivatives of the CAS spectra are also shown. PL spectra recorded at 2 K at low excitation densities are also shown for comparison. For the 3-Å GaSb superlattice the PL peak energy agrees with the calculated one for a transition between an electron in the GaAs layer and a heavy hole confined in the GaSb layer (see Fig. 5). Despite different energies of their characteristic features, both CAS spectra look *qualitatively* similar. Note that no peak in the absorption spectrum can be resolved at an energy corresponding to the GaSb-related luminescence peak, as anticipated from the small value of the exciton binding energy and the low expected absorption coefficient at the band edge. However, the absorption starts just in the very vicinity of the PL peak, indicating that it is of intrinsic origin. This is additionally manifested by a clearly resolved positive peak in the second derivative of the CAS spectrum (CAS") which characterizes the onset of the absorption and coincides with the PL peak. We note that the second derivative analysis is a powerful method for evaluation of PL, PLE, and absorption data when the features in the original spectra are strongly modified by broadening, overlapping of different peaks, and (or) superimposed on background signals. Change in a CAS" spectrum from 0 to positive, then to negative, and then back to positive indicates a peak in the original spectrum.

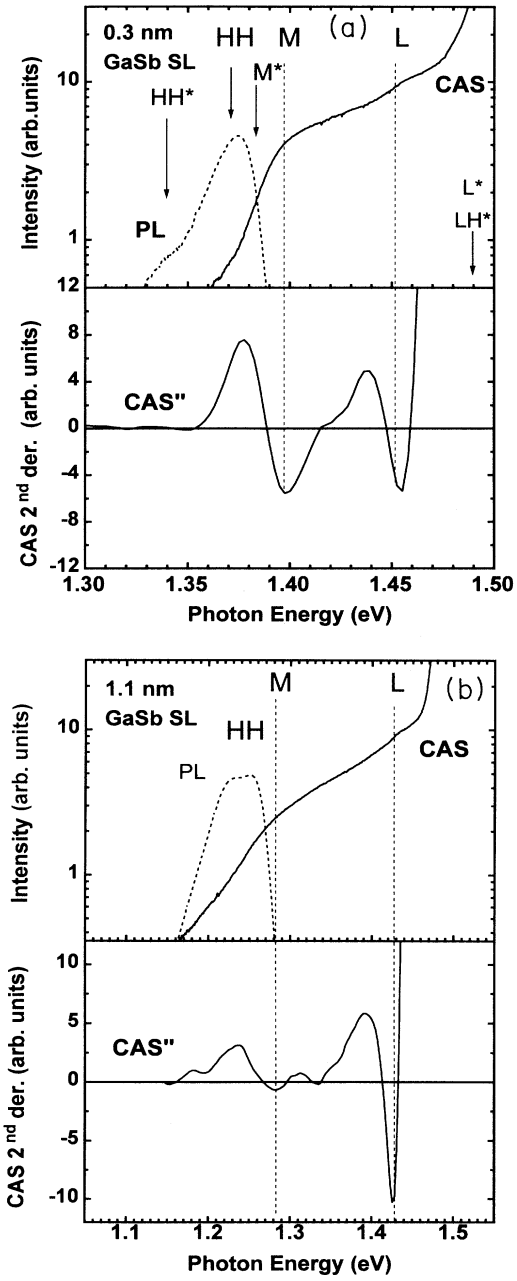

FIG. 7. (a) Calorimetric absorption spectrum (CAS) of a superlattice having 3 Å GaSb layers, second derivative of the CAS spectrum, and low excitation density low-temperature ($T=2$ K) PL spectrum. Calculated energies for GaSb heavy-hole–GaAs electron (HH*) and GaSb light-hole–GaAs electron (LH*) transitions, as well as for valence-band mixing-induced singularities (M^*,L^*) are shown by the arrows. (b) Calorimetric absorption spectrum (CAS) of a superlattice having 11-Å GaSb layers, second derivative of the CAS spectrum, and low excitation density low-temperature ($T=2$ K) PL spectrum (note the logarithmic scale).

One can see two clearly distinguished minima in the CAS" spectra, where the second derivative becomes negative: at energies M and L. These characteristic features can also be resolved in both original CAS spectra. For the 3-Å GaSb superlattice the energy position of the higher-energy feature (L) is relatively close to the energy expected for a transition between an electron located in the GaAs layer and a light hole localized in the GaSb layer. Feature M lies at energies between heavy- and light-hole-related transitions. At the same time, as was mentioned already, any heavy- or light-hole exciton peaks are excluded in a strongly type-II GaSb/GaAs system, as follows from Fig. 3. Possible broadening mechanisms, e.g., due to GaSb layer width fluctuations, can result only in the smearing out of sharp features, but cannot explain their appearance in the spectra. There is another feature resolved in CAS" spectra on the high-energy side of the M peak. However, it is much weaker and the sign of the second derivative is not clearly negative at these energies; thus one can attribute this feature to the change in the slope in the original CAS spectrum rather than to a separate peak.

To learn more about the peculiarities of the joint density of states in type-II GaSb-GaAs structures, we studied the temperature dependence of the photoluminescence spectra: the PL spectra at different temperatures, the shift of the PL peak energy with rising observation temperature, and the dependence of the logarithm of the integrated intensity versus reciprocal temperature are shown in Figs. 8(a), 8(b), and 8(c), respectively. A 3-Å GaSb/GaAs superlattice was studied. An activation energy derived from the slope of the integrated intensity versus inverse temperature was found to be ~170 meV, in good agreement with the total-energy difference between the GaAs band gap and the GaSb-related PL peak energy. This observation agrees with the fact that the entire energy shift originates from the localization of holes.

This situation is different from the case of InAs/GaAs structures, where both electrons and holes are localized and contribute to the total PL line shift, and the activation energy is smaller than the PL line energy separation with respect to the GaAs band-gap energy.

Two regions can be clearly resolved in the temperature dependence of the PL peak energy [Fig. 8(c)]: for lower temperatures (up to ~150 K) the PL peak does not significantly change its spectral position, and thus the PL maximum shifts to higher photon energies relative to the effective band-gap energy. This can be easily explained by the thermal population of electron and hole states with high-k values having a higher probability of radiative recombination.[23] This behavior is expected for type-II quantum wells, where the band-to-band absorption coefficient near the effective band gap is proportional to $(\hbar\omega-\hbar\omega_0)^{3/2}=\varepsilon^{3/2}$.[23] Assuming the Boltzmann distribution of nonequilibrium carriers and the band-to-band origin of radiative recombination, the PL peak energy should follow the $E_g^*(T)+3/2kT$ dependence. According to this formula for temperatures close to 150 K the total shift of the PL line with respect to the effective band gap should be equal to ~20 meV, in good agreement with experimental observation [see Fig. 8(c)]. However, for temperatures above 150–170 K the behavior of the PL peak changes, and it follows the band gap exactly.[24] This is expected for band-to-band transitions in type-I quantum-well structures having a steplike joint density of states, or for exciton luminescence in bulk semiconductors, where zero-phonon radiative recombination is possible only in the very vicinity of $E_g^*(T)$ (the exciton polariton region). Thus the characteristic difference in the PL line temperature shift for the two temperature regions points to a thermal population of the states providing a much higher optical transition matrix element than ones in the vicinity of $k=0$, and exhibiting *qualitatively* different (type-I) behavior in the *joint density of states.*

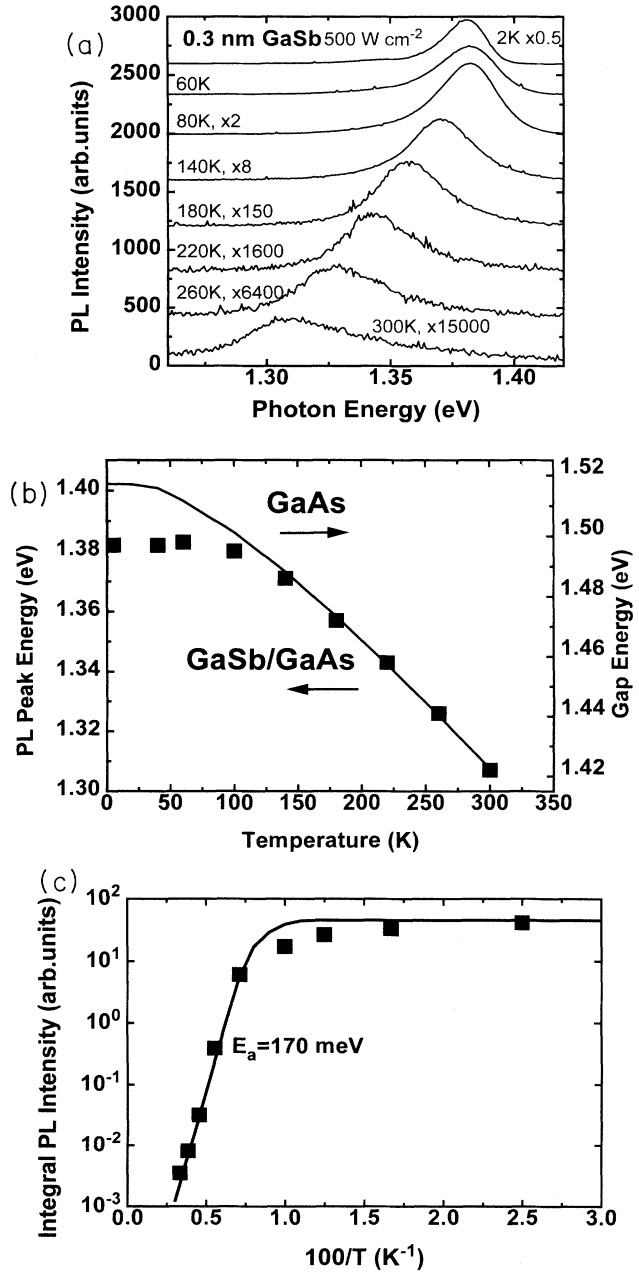

FIG. 8. (a) PL spectra of a 3-Å GaSb superlattice recorded at different observation temperatures. (b) PL peak energy dependence on the observation temperature. (c) Logarithm of the integrated PL intensity vs reciprocal temperature together with the activation energy fit.

We should pay attention to the energy difference between the absorption feature denoted by M in Fig. 7(b) (characterizing the transition to a more steplike behavior of the absorption spectrum) and the heavy-hole peak in the PL spectrum. This difference approximately equals 25 meV, and agrees with the *total-energy* shift of the luminescence line with respect to the effective band-gap energy when the observation temperature is increased [see Fig. 8(c)].

We consider possible mechanisms responsible for the optical properties observed. For ultrathin GaSb/GaAs structures, there exist only one GaSb heavy-hole subband and only one light-hole subband, and these subbands are well separated. Thus the system may be treated as a model one. As the quasi-3D-like electron density of states is essentially featureless, the effect observed involves the GaSb valence-band. Features (Denoted by M and L in Fig. 7) in the absorption spectrum can be attributed to heavy- and light-hole mixing effects in the continuum of the quantum-well valence band. The valence-band mixing effects[25–29] are known to result in light in-plane effective masses for the heavy-hole subband, and in heavy-hole-like (or even electronlike) in-plane effective masses for the light-hole subband near $k\approx 0$. These effects also result in singularities in the density of hole states in the continuum of the heavy-hole subband and at the top of the light-hole subband.[26] The origin of the heavy-hole subband singularity may be explained qualitatively as follows: at some characteristic k_0 value the light-hole-like in-plane heavy-hole subband effective mass increases. This bending gives rise to a peak in the heavy-hole subband density of states and also in the exciton density of states[26] (exciton absorption for $k>0$ is possible

in ultrathin quantum wells if interface corrugation partly lifts the k-selection rules). For the same k_0 value the *perpendicular* hole mass *decreases,* resulting in an effective *delocalization* of the heavy-hole wave function, increasing electron and hole wave function overlap.

The singularity in the light-hole subband (L) *remains* in the *joint* density of states, due to positive (electronlike) light-hole effective mass for small $k_{x,y}$ values. We emphasize that this singularity is *not* connected with the excitonic effect, and entirely originates from band-to-band transitions. Contrary to this, the heavy-hole singularity is partly *smeared out* in the band-to-band absorption spectrum due to large electron dispersion,[26,30] resulting in a more *smooth* absorption profile. For type-I quantum wells, the valence-band mixing effects do not play an important role in absorption and PL spectra, as the ground-state exciton contributions are dominant in both cases. Conversely, for ultrathin staggered line-up quantum wells these effects can have a strong influence on the optical properties.

The alternative explanation can include exciton or exciton continuum effects involving virtual s-exciton states expelled into the absorption continuum. However, the energy of these states is extremely sensitive to the average GaSb layer thickness as it follows from Fig. 3. This is not supported by the experimental results (see Fig. 7).

Based on the investigations presented, interesting applications are to be expected. By appropriate selection of a type-II structure geometry one can tune the radiative state energy to be closed to the absorption onset. In this case the geometry may be thermally populated, resulting in an efficient radiative recombination up to room temperature. We found that in the case of a five-period 1-ML GaSb–2-ML GaAs superlattice symmetrically confined from both sides with five-period GaAs/$Al_{0.4}Ga_{0.6}$As superlattices with layer thicknesses of 20 Å and, subsequently, by 200-Å-thick $Al_{0.4}Ga_{0.6}$ As layers, the integral luminescence intensity depends relatively weakly on the lattice temperature particularly at high excitation densities (the integral PL intensity drops by only three times at 500 W cm^{-2} in a 8–300-K temperature range). The temperature dependence of the PL-spectrum of this structure at low excitation densities is shown in Fig. 9. The PL intensity at room temperature is similar to that of a reference type-I GaAs/(Al,Ga)As single-quantum-well structure grown with the same deposition conditions and with similar (Al,Ga)As cladding layers.

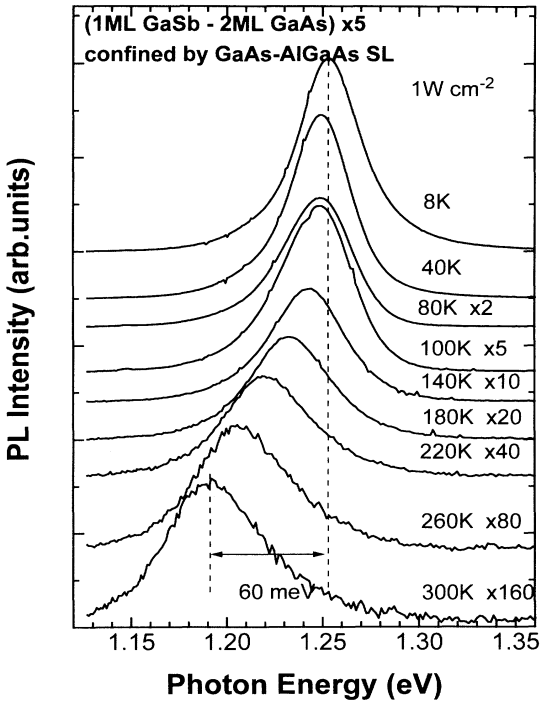

FIG. 9. PL spectra of a short-period 1-ML GaSb–2-ML GaAs superlattice, composed of five periods and symmetrically confined from both sides by a five-period GaAs/$Al_{0.4}Ga_{0.6}$As superlattice with layer thicknesses of 20 Å and, subsequently, by 200-Å-thick $Al_{0.4}Ga_{0.6}$As layers. Only a moderate decrease of PL intensity with temperature increase is observed, even at very low excitation densities, contrary to Figs. 8(a) and 8(c).

V. CONCLUSIONS

We investigated the optical properties of ultrathin GaSb quantum wells grown in a GaAs matrix by molecular-beam epitaxy. PL, calorimetric absorption, and time-resolved PL studies support the type-II nature of the GaSb/GaAs heterostructure. A pronounced change in the character of the absorption spectra is observed for heavy holes, in particular at $k^*_{x,y} > 0$. This change is in agreement with the different behavior of the PL line shift at low and high temperatures of observation. We attribute these observations to heavy- and light-hole mixing effects in the continuum of the GaSb quantum-well valence band. By appropriate selection of the type-II structure geometry, we demonstrate a tuning of its optical properties, approaching the radiative efficiency of type-I quantum wells. The effects observed are expected to be important for far-infrared light-emitting device engineering (e.g., based on the InAs/GaSb system).

ACKNOWLEDGMENTS

This work is supported by Volkswagen-Stiftung, by Grant No. INTAS-94-1028, and by Deutsche Fortschungsgemeinschaft in the framework of Sfb 296. N.N.L. is grateful to the Alexander von Humboldt Foundation.

*On leave from A. F. Ioffe Physical-Technical Institute, St. Petersburg, Russia.

[1]H. Kroemer and G. Griffiths, IEEE Electron Device Lett. **EDL4**, 20 (1983).

[2]P. Voisin, G. Bastard, C. E. T. Gonçalvés de Silva, M. Voos, L. L. Chang, and L. Esaki, Solid State Commun. **39**, 79 (1981).

[3]J. Böhrer, A. Krost, D. Bimberg, M. Helm, and G. Bauer, Appl. Phys. Lett. **63**, 2955 (1993).

[4]A. N. Baranov, B. E. Dzhurtanov, A. N. Imenkov, A. A. Rogachev, Yu. M. Shernyakov, and Yu. P. Yakovlev, Fiz. Tekh. Polopruvodn. **20**, 2117 (1986) [Sov. Phys. Semicond. **20**, 1385 (1986)].

[5]A. N. Titkov, Yu. P. Yakovlev, A. N. Baranov, and V. N. Cheban, in *Proceedings of the 20th International Conference on the Physics of Semiconductors, Thessaloniki, Greece, 1990,* edited by E. M. Anastassakis and J. D. Joannopoloulos (World Scientific, Singapore, 1990), p. 985.

[6]R. Zimmerman and D. Bimberg, J. Phys. (France) IV **3**, C261 (1993).

[7]L. L. Chang, J. Phys. Soc. Jpn. **49**, Suppl. A, 997 (1980).

[8]G. A. Sai-Halasz, L. L. Chang, J. M. Welter, C.-A. Chang, and L. Esaki, Solid State Commum. **27**, 935 (1978).

[9]P. Voisin, Y. Guldner, J. P. Vieren, M. Voos, C. Benoit a la Guillaume, N. J. Kawai, L. L. Chang, and L. Esaki, J. Phys. Soc. Jpn. **49**, Suppl. A, 1005 (1980).

[10]R. H. Miles, D. H. Chow, J. N. Schulman, and T. C. McGill, Appl. Phys. Lett. **57**, 801 (1990).

[11]G. Bastard, E. E. Mendez, L. L. Chang, and L. Esaki, Phys. Rev. B **26**, 1974 (1982).

[12]J. M. Rorison, Phys. Rev. B **48**, 4643 (1993).

[13]A. Juhl and D. Bimberg, J. Appl. Phys. **64**, 303 (1988).

[14]D. Bimberg, T. Wolf, and J. Böhrer, in *Advances in Nonradiative Processes in Solids,* edited by B. di Bartolo (Plenum, New York, 1991), p. 577.

[15]T. S. Argunova, R. N. Kyutt, S. S. Ruvimov, and M. P. Scheglov, in *Microscopy of Semiconducting Materials,* edited by A. G. Cullis and N. J. Long, IOP Conf. Proc. No. 117 (Institute of Physics, London, 1991), Sect. 9, p. 669.

[16]C. G. van de Walle, Phys. Rev. B **39**, 1871 (1989).

[17]M. P. C. Krijn, Semicond. Sci. Technol. **6**, 27 (1991).

[18]*Semiconductors Physics of Group IV Elements and III-V Compounds,* edited by K.-H. Hellwege and O. Madelung, Landolt-Börnstein, New Series, Group III, Vol. 17, Pt. a (Springer-Verlag, Berlin, 1982).

[19]I. Yassievich, U. Roessler, J. Phys. Condens. Matter **6**, 7927 (1994); P. D. Wang, N. N. Ledentsov, C. M. Sotomayor Torres, I. N. Yassievich, A Pakhomov, A. Yu. Egorov, P. S. Kop'ev, and V. M. Ustinov, Phys. Rev. B **50**, 1604 (1994).

[20]M. S. Bressler, O. B. Gusev, M. P. Mikhailova, V. V. Sherstnev, Yu. P. Yakovlev, and I. N. Yassievich, Fiz. Tekh. Polopruvodn. **25**, 298 (1991) [Sov. Phys. Semicond. **25**, 181 (1991)].

[21]C. Weisbuch, B. Vinter, *Quantum Semiconductor Structures* (Academic, Boston, 1991), p. 20.

[22]F. Hatami, N. N. Ledentsov, J. Böhrer, M. Grundmann, D. Bimberg, S. S. Ruvimov, P. Werner, U. Gösele, J. Heydenreich, S. V. Ivanov, P. S. Kop'ev, and Zh. I. Alferov, Appl. Phys. Lett. **67**, 656 (1995).

[23]G. Bastard, *Wave Mechanics Applied to Semiconductor Heterostructures* (Les Editions de Physique, Paris 1988).

[24]C. D. Thurmond, J. Electrochem. Soc. **122**, 1133 (1975).

[25]U. Ekenberg and M. Altarelli, Phys. Rev. B **32**, 3712 (1985).

[26]M. Altarelli, U. Ekenberg, and A. Fasolino, Phys. Rev. B **32**, 5138 (1985).

[27]L. C. Andreani, A. Pasquarello, and F. Bassani, Phys. Rev. B **36**, 5887 (1987).

[28]G. Platero and M. Altarelli, Phys. Rev. B **36**, 6591 (1987).

[29]M. Altarelli, in *Heterostructures and Semiconductor Superlattices,* edited by G. Allan, G. Bastard, M. Boccara, M. Lannoo, and M. Voos (Springer-Verlag, Berlin, 1986), p. 12.

[30]D. Hessman, M.-E. Pistol, J. Olajos, and L. Samuelson, Phys. Rev. B **49**, 17 118 (1994).